

Interdomain Interaction Reconstitutes the Functionality of PknA, a Eukaryotic Type Ser/Thr Kinase from *Mycobacterium tuberculosis**

Received for publication, September 10, 2007, and in revised form, January 14, 2008. Published, JBC Papers in Press, January 16, 2008, DOI 10.1074/jbc.M707535200

Meghna Thakur¹, Rachna Chaba², Alok K. Mondal, and Pradip K. Chakraborti³

From the Institute of Microbial Technology, Sector 39A, Chandigarh 160 036, India

Eukaryotic type Ser/Thr protein kinases have recently been shown to regulate a variety of cellular functions in bacteria. PknA, a transmembrane Ser/Thr protein kinase from *Mycobacterium tuberculosis*, when constitutively expressed in *Escherichia coli* resulted in cell elongation and therefore has been thought to be regulating morphological changes associated with cell division. Bioinformatic analysis revealed that PknA has N-terminal catalytic, juxtamembrane, transmembrane, and C-terminal extracellular domains, like known eukaryotic type Ser/Thr protein kinases from other bacteria. To identify the minimum region capable of exhibiting phosphorylation activity of PknA, we created several deletion mutants. Surprisingly, we found that the catalytic domain itself was not sufficient for exhibiting phosphorylation ability of PknA. However, the juxtamembrane region together with the kinase domain was necessary for the enzymatic activity and thus constitutes the catalytic core of PknA. Utilizing this core, we deduce that the autophosphorylation of PknA is an intermolecular event. Interestingly, the core itself was unable to restore the cell elongation phenotype as manifested by the full-length protein in *E. coli*; however, its co-expression along with the C-terminal region of PknA can associate them in *trans* to reconstitute a functional protein *in vivo*. Therefore, these findings argue that the transmembrane and extracellular domains of PknA, although dispensable for phosphorylation activities, are crucial in responding to signals. Thus, our results for the first time establish the significance of different domains in a bacterial eukaryotic type Ser/Thr kinase for reconstitution of its functionality.

Signal transduction in living organisms plays a pivotal role in controlling several aspects of cellular processes such as metabolism, cell growth, cell motility, cell division, and differentiation. These processes need to be tightly regulated to ensure signaling fidelity, and this synchronization in eukaryotes is

mediated primarily through phosphorylation of serine, threonine, and/or tyrosine residues catalyzed by protein kinases. Although they exhibit similarities in their catalytic domains, different kinases may contain additional regions, allowing a multitude of mechanisms for their control. The role of these Ser/Thr or Tyr protein kinases in eukaryotic signal transduction is well established and widely documented (1). Considerably less is known about the prevalence and role of these protein kinases in bacteria and Archaea, where phosphorylation events are predominantly materialized by two-component His kinases along with response regulators, which do not share any sequence similarity with Ser/Thr or Tyr kinases (2). In fact, in the advent of genome sequencing, the presence of genes encoding eukaryotic type Ser/Thr protein kinases in diverse bacterial species raises the possibility of their indispensable involvement in complex network of signal transduction cascade. Although the phosphorylation of these bacterial kinases has been intensively established, the experimental proof of their physiological function and regulation is scarce. Thus, a detailed study of eukaryotic type kinases in bacteria is indeed essential to have insights on their contribution to signaling events. In this context, we focused on the dreadful pathogen *Mycobacterium tuberculosis*, the causative agent of tuberculosis. The medical impact of tuberculosis (3), which infects nearly one-third of the world's human population causing considerable mortality annually, therefore provides the rationale for investigating these regulatory proteins in the signaling process.

The genome of *M. tuberculosis* has unveiled the presence of a family of 11 eukaryotic type Ser/Thr kinases (4). All of these kinases, except PknG and PknK, encode predicted receptors with a single transmembrane helix dividing the protein into N-terminal intracellular and C-terminal extracellular domains (5). Unlike most of the eukaryotes, the N terminus contains a kinase domain, which is linked to the transmembrane region through a variable length of juxtamembrane linker (6). The C-terminal domain outside the cell presumably binds signaling ligands and is attached to the transmembrane sequence. The architecture of these eukaryotic type kinases is very similar throughout bacteria and typical of receptor-like kinases in plants (7). Majority of them (PknA, PknB, PknD, PknE, PknF, PknG, PknH, PknI, and PknL) have been shown to catalyze autophosphorylation and substrates for few of them have been identified (8–18). Besides, the crystal structure of the catalytic domain of PknB was solved, which provided valuable information regarding the regulatory mechanism of this kinase (19, 20).

* This work was supported in part by a network project grant from the Council of Scientific and Industrial Research. The costs of publication of this article were defrayed in part by the payment of page charges. This article must therefore be hereby marked "advertisement" in accordance with 18 U.S.C. Section 1734 solely to indicate this fact.

¹ Recipient of a senior research fellowship from the Council of Scientific and Industrial Research, New Delhi, India.

² Present address: Dept. of Microbiology and Immunology, University of California, San Francisco, CA 94158.

³ To whom correspondence should be addressed. Tel.: 91-172-2690751; Fax: 91-172-2690585; E-mail: pradip@imtech.res.in.

Sepharose 4B affinity column, and protein was eluted with lysis buffer containing 10 mM glutathione. For use as controls, in similar manner MBP- β gal/GST proteins were prepared and purified from *E. coli* cells transformed with vectors.

Kinase Assay—The ability of autophosphorylation and substrate phosphorylation of PknA or its mutants as purified fusion proteins was determined in an *in vitro* kinase assay. Aliquots (usually 1 μ g/20 μ l reaction volume) of fusion protein were mixed with 1 \times kinase buffer (50 mM Tris-Cl, pH 7.5, 50 mM NaCl, 10 mM MnCl₂), and the reaction was initiated by adding 2 μ Ci of [γ -³²P]ATP. Following incubation at room temperature for 20 min, the reaction was stopped by adding SDS sample buffer (30 mM Tris-Cl, pH 6.8, 5% glycerol, 2.5% β -mercaptoethanol, 1% SDS, and 0.01% bromophenol blue). Samples were boiled for 5 min and resolved on 8–12.5% SDS-PAGE. Gels were stained with Coomassie Brilliant Blue, dried in a gel dryer (Bio-Rad) at 70 °C for 2 h, and analyzed in a phosphorimaging device (Molecular Imager FX, Bio-Rad) and also exposed to x-ray films (Eastman Kodak Co.).

Co-transformation—*E. coli* (strain DH5 α) cells were co-transformed with two incompatible plasmids, pMAL/pGEX-KG and p19Kpro, harboring different constructs. The presence of different antibiotic selections (ampicillin in pMAL/pGEX and hygromycin in p19Kpro) facilitated the co-expression of foreign proteins in *E. coli* using these incompatible plasmids (21, 23). The *E. coli* cells harboring pMAL or pGEX with gene(s) of interest were grown in the presence of ampicillin (100 μ g/ml) and made competent using standard methods (24). The cells were then transformed with p19Kpro containing the desired gene(s) and plated on LB agar with both ampicillin (75 μ g/ml) and hygromycin (200 μ g/ml). Clones obtained were cultured in LB broth in the presence of both the antibiotics and induced with 0.2 mM IPTG (37 °C/3 h). Cells were further processed for microscopy or Western blotting.

Western Blotting—Purified fusion proteins (~800 ng) or samples obtained in co-transformation experiments were resolved in 8–10% SDS-PAGE and transferred at 250 mA for 45 min to nitrocellulose membrane (0.45 μ m) in a mini-transblot apparatus (Bio-Rad) using Tris-glycine-SDS buffer (48 mM Tris, 39 mM glycine, 0.037% SDS, and 20% methanol, pH ~ 8.3). Primary antibodies (anti-MBP from New England Biolabs and anti-Thr(P) from Cell Signaling Technology) used for different immunoblots were either commercially available (New England Biolabs) or raised as mentioned elsewhere (9). Horseradish peroxidase-conjugated anti-rabbit IgG secondary antibody (GE Healthcare) was chosen depending on the primary antibody used and subsequently processed with the ECL detection system (GE Healthcare) following the manufacturer's recommended protocol.

Pulldown Assay—Purified fusion proteins (GST-(253/363), GST-(363/431), GST-(Δ 1–252) and MBP-Core; 100 μ g of each protein/reaction) were mixed in 600 μ l of binding buffer (200 mM NaCl, 1 mM EDTA in 20 mM Tris-Cl, pH 8) and incubated for 1 h at 4 °C with gentle mixing. This was followed by the binding reaction (1 h at 4 °C) in the presence of amylose beads (25 μ l) and glutathione (final concentration of 10 mM to avoid nonspecific binding of GST to amylose resin). Following washing of beads (five times with binding buffer containing 0.1%

Tween 20; 1 ml/wash), the resin-bound proteins were extracted and subsequently processed for Western blotting using anti-GST/anti-MBP antibody.

Solid Phase Interaction Assay—The association between purified GST and MBP fusion proteins was identified by solid phase interaction assay as described elsewhere (20). Briefly, purified MBP-Core after dialysis against PBS was incubated (2 h at 25 °C with gentle mixing) with 10-fold molar excess of biotin-NHS. The mixture was extensively dialyzed and used as a source of biotinylated protein after estimation (25). For binding studies, different GST constructs (GST-(253/363), GST-(363/431), and GST-(Δ 1–252); 1 μ g/well) were coated in microtiter plates for 3 h at 37 °C. Following washing with PBS containing 0.5% Tween (PBS-T), the wells were blocked with 1% BSA in PBS-T for 1 h at 37 °C. After extensive washing with PBS-T, the wells were incubated (1 h at 37 °C) with different concentrations of biotinylated MBP-Core. The interaction was finally monitored by addition of streptavidin-HRP (1 μ g/ml for 30 min at 37 °C), and enzyme activity in each well was detected using 3,3',5,5'-tetramethylbenzidine as the substrate. Binding of biotinylated core with immobilized Δ 1–252 was assessed in the presence of different concentrations of nonbiotinylated Δ 1–252 to determine the specificity of the interaction. In each case, for controls instead of fusion proteins an equivalent amount of BSA was adsorbed to the wells of microtiter plates.

Bioinformatic Analysis—The multiple sequence alignment of the protein sequences retrieved from the mail server at the National Institutes of Health was carried out using the ClustalX1.81 program (26). Secondary structure of the protein was predicted using PSIPRED server (27), and for tertiary structure prediction an automated protein homology-modeling server "Swiss Model" was used (28). Using LSQMAN (Least Square Manipulation; see Ref. 29), the predicted structure of PknA was superimposed with that of the PknB structure, which has been complexed with nucleotide triphosphate analog. For 260 C α atoms the root mean square deviation was 0.47 Å. The superimposed structure was generated using PyMOL (30).

Microscopy—*E. coli* (strain DH5 α) cells transformed/co-transformed with different plasmid constructs (p19kpro-Core, pMAL-253/363, pMAL-363/431, and pMAL- Δ 1–252) were reinoculated at an initial A_{600} of 0.05 and grown further for 12 h. Because there was leaky expression of the MBP fusion proteins (pMAL-253/363, pMAL-363/431, and pMAL- Δ 1–252), the cultures were not induced with IPTG. Cells were harvested by centrifugation and subjected to fixation with ethanol after washing with PBS. The fixed cells were collected by centrifugation and resuspended in PBS. The cells were spread on poly-L-lysine-coated glass slides and examined under microscope (Carl Zeiss) following staining with 1% methylene blue solution.

RESULTS

Kinase Domain Together with the Juxtamembrane Region Constitutes the Catalytic Core of PknA—Analysis of the nucleotide-derived amino acid sequence of PknA indicated the presence of a highly conserved catalytic domain, followed immediately by a juxtamembrane region rich in alanine and proline. The juxtamembrane region leads to a hydrophobic stretch of 23 amino acids constituting the putative transmembrane and the

Self-association of PknA Reconstitutes Its Functionality

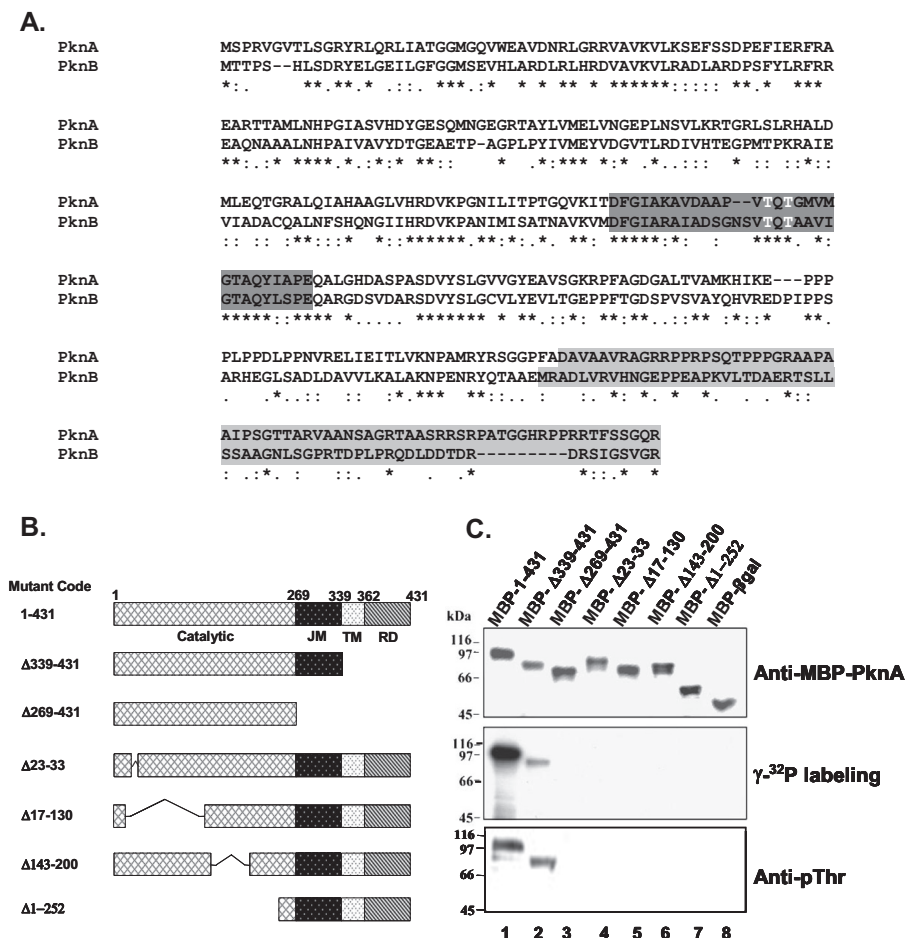


FIGURE 1. Deletion analysis of PknA. *A*, pairwise alignment of amino acid sequence of *M. tuberculosis* PknA with another Ser/Thr kinase PknB located in the same operon. Nucleotide-derived amino acid sequences of the PknA (residues 1–338) and PknB (residues 1–331) encompassing the catalytic domain and the putative juxtamembrane region were aligned using ClustalX1.81 program. The juxtamembrane region and the activation loop have been shaded in light and dark gray, respectively. Threonine residues (Thr-172 and Thr-174) within the activation loop are highlighted in white. *B*, schematic diagram of various deletion mutants of PknA as described under “Experimental Procedures.” Δ followed by numbers indicate the deleted regions. Abbreviations used are as follows: JM, juxtamembrane region; TM, transmembrane region; RD, regulatory domain. *C*, autophosphorylation ability of the deletion mutants of PknA. Western blot analysis with rabbit polyclonal anti-MBP-PknA sera (anti-MBP-PknA, upper panel), γ - 32 P labeling (middle panel), and immunoblotting with anti-phosphothreonine antibody (anti-pThr, lower panel) of different deletion mutants of PknA. Lane numbers are shown at the bottom. Position of molecular mass markers is indicated.

C-terminal extracellular domain. On aligning the sequence with PknB, another mycobacterial Ser/Thr kinase located adjacent to the PknA in the genome and with known crystal structure, the catalytic domain was found to be highly homologous (~78% homology with ~42% identity). Furthermore, the predicted secondary structure (using “PSIPRED” server) and the modeled tertiary structure of PknA (using the “Swiss-Model”) catalytic domain revealed a remarkably high similarity with PknB. However, the homology between the juxtamembrane regions of these two kinases was considerably less (~47% homology with ~15% identity) (Fig. 1A). Because the catalytic domain in PknB is sufficient for autophosphorylation as well as substrate phosphorylation (31), it was intriguing to know whether the catalytic domain alone of PknA could perform a similar function. To have insight on this aspect, several deletion mutations were constructed as outlined in Fig. 1B. The deletion mutants were purified as MBP fusion proteins, and expression was confirmed by immunoblot analysis with the rabbit poly-

clonal antisera against MBP-PknA (Fig. 1C, upper panel). The autophosphorylating status of the deletion mutants was analyzed by an *in vitro* kinase assay (Fig. 1C, middle panel) and further confirmed by immunoblotting with anti-Thr(P) antibody (Fig. 1C, lower panel). On analyzing the kinase activity, we found that only the Δ 339–431 deletion mutant of PknA harboring the catalytic domain and juxtamembrane region retained the autophosphorylating ability. However, unlike PknB, further shortening of this domain (Δ 269–431) by deleting the putative juxtamembrane region completely abolished the kinase activity (Fig. 1C, middle panel). This observation was further supported by the fact that anti-phosphothreonine antibody recognized only the Δ 339–431 protein among all mutants and MBP β -galactosidase control (Fig. 1C, lower panel). Thus our results argue that the catalytic domain along with the juxtamembrane region (residues 1–338) are required for PknA autophosphorylation, and hereafter we designate the mutant as the “core” of PknA.

The boundary of the catalytic domain was identified on the basis of primary sequence alignment. However, on careful analysis of the predicted secondary structure and tertiary structures of PknA, using PknB as template, it was found that the Δ 269–431 deletion construct missed more than half of the α 1

helix, which has been found to be involved in a four-helix bundle in PknB (20). As can be seen in Fig. 2A, the superimposed structure of PknA with PknB highlights the presence of a helix (α 1) toward the end of the catalytic domain. The boundary of the helix was further marked by analyzing the predicted secondary structure of PknA (Fig. 2A, inset), and it extended to VRAG (ending at residue 277) corresponding to VHNG (ending at residue 279) in PknB (Fig. 1A). Therefore, to analyze the role of this region in the activity of PknA, another deletion mutant, Δ 278–431 (retaining the helix), was constructed. The mutant was tested for its autophosphorylation ability by *in vitro* kinase assay as well as immunoblotting with anti-Thr(P) antibody. As shown in Fig. 2B, no incorporation of γ - 32 P occurred even with 10 μ g of the Δ 278–431 mutant; however, 2.5 μ g of the Δ 339–431 mutant (core) exhibited phosphorylation (compare lanes 2, 4, and 6). This observation was further supported by immunoblotting anti-Thr(P) antibody, which did not recognize the Δ 278–431 mutant (Fig. 2C, lane 2). These observa-

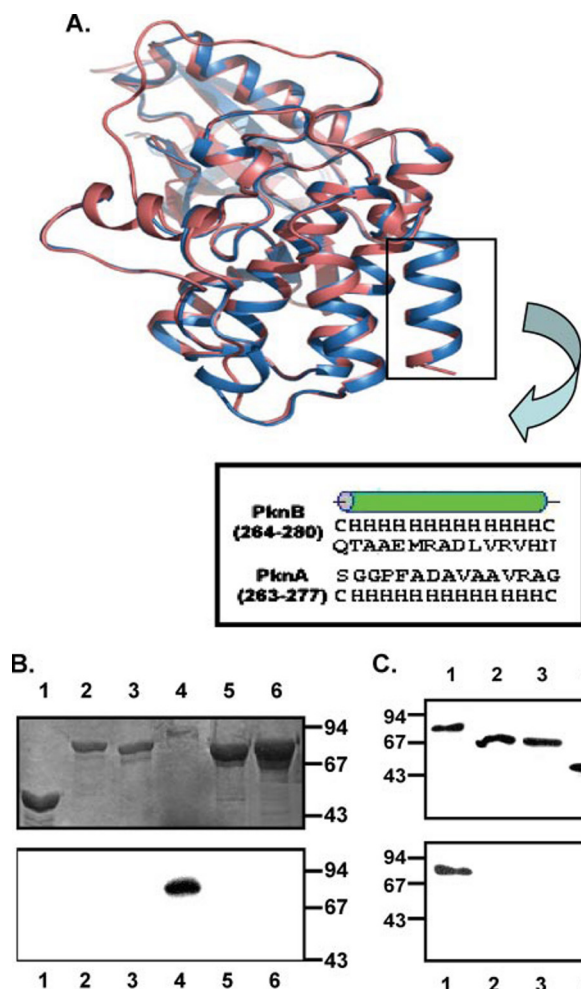


FIGURE 2. Model of PknA catalytic domain superimposed on PknB. A, amino acid residues 1–273 of PknA modeled using Swiss-Prot were superimposed on the structure of PknB (residues 1–279). *Inset*, secondary structure prediction of the last helix α -helix (α) of the catalytic domain of PknA and PknB highlighting the boundary of the helix. B, γ - 32 P labeling of deletion mutants of the catalytic domain of PknA. A representative experiment showing Coomassie-stained gel (*upper panel*) and the autoradiogram (*lower panel*) of MBP- β -gal (*lane 1*, 5 μ g), MBP-(Δ 278–431) (*lane 2*, 2.5 μ g, and *lane 6*, 10 μ g), MBP-(Δ 269–431) (*lane 3*, 2.5 μ g, and *lane 5*, 10 μ g) and MBP-Core (*lane 4*, 2.5 μ g) following incubation with [γ - 32 P]ATP as described under “Experimental Procedures” under kinase assay. C, Western blotting of MBP-Core (*lane 1*), MBP-(Δ 278–431) (*lane 2*), MBP-(Δ 269–431) (*lane 3*), and MBP- β -gal (*lane 4*) using anti-MBP-PknA (*upper panel*) and anti-pThr (*lower panel*) antibodies. In each case 1 μ g of protein was loaded. Lane numbers are shown at the top and bottom. Position of molecular mass markers is indicated.

tions thus established that, unlike PknB, the catalytic domain alone was insufficient for phosphorylation in PknA.

The Core Mimics the Catalytic Activities of PknA—To examine the autophosphorylation pattern of the core, *in vitro* phosphorylation assays were carried out. The core was capable of phosphorylating itself in a concentration-dependent manner like the full-length PknA, although 5 μ g of the protein exhibited phosphorylation comparable with 800 ng of full-length protein (Fig. 3A) (9). Furthermore, the effect of divalent cations was also concomitant with full-length PknA, as autophosphorylation was detectable only in the presence of Mn^{2+} and to some extent with Mg^{2+} (Fig. 3B). Similarly, the potent kinase inhibitors (ammonium molybdate, sodium tungstate, and sodium vanadate) affected the phosphorylation of the core (Fig. 3C). All

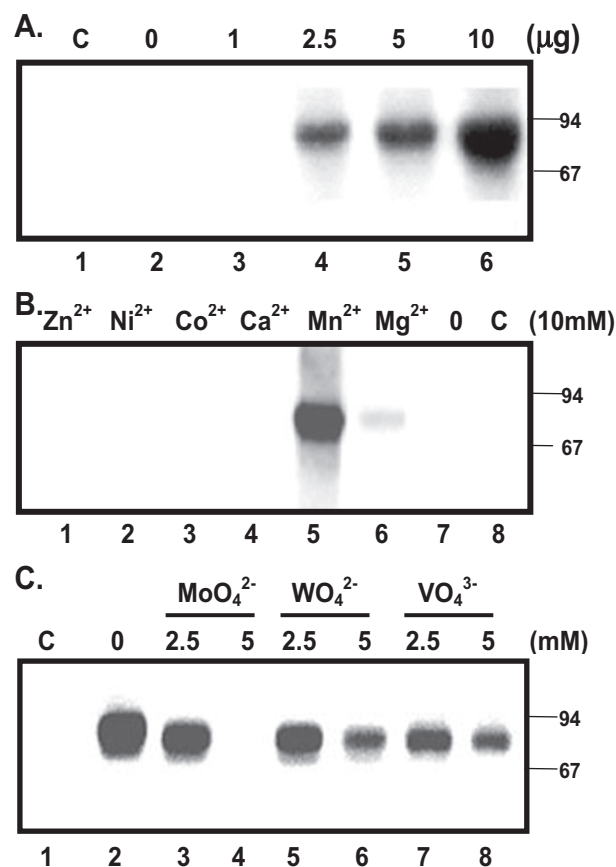


FIGURE 3. Autophosphorylation of PknA core. Autophosphorylation of the PknA core was monitored by incubating purified protein with [γ - 32 P]ATP followed by separation of the reaction products by SDS-PAGE. The labeled proteins were visualized in a phosphorimaging device or by autoradiography of the dried gel (see “Experimental Procedures”). A, autophosphorylation with 0 (*lane 2*), 1 (*lane 3*), 2.5 (*lane 4*), 5 (*lane 5*), and 10 μ g (*lane 6*) of purified MBP-Core along with 5 μ g of heat-inactivated protein (*lane 1*) in the presence of 10 mM Mn^{2+} . B, effect of divalent cations. Autophosphorylation of core (5 μ g of protein/reaction) was carried out in the presence of 10 mM of Zn^{2+} (*lane 1*), Ni^{2+} (*lane 2*), Co^{2+} (*lane 3*), Ca^{2+} (*lane 4*), Mn^{2+} (*lane 5*), Mg^{2+} (*lane 6*), or absence (*lane 7*) of ions and boiled protein (*lane 8*) in the presence of 10 mM Mn^{2+} . C, effect of different inhibitors. *Lane 1*, boiled protein; *lane 2*, no inhibitor; *lane 3*, 2.5 mM ammonium molybdate; *lane 4*, 5 mM ammonium molybdate; *lane 5*, 2.5 mM sodium tungstate; *lane 6*, 5 mM sodium tungstate; *lane 7*, 2.5 mM sodium vanadate; *lane 8*, 5 mM sodium vanadate.

these results therefore strongly suggest that the autophosphorylation behavior of the core mimics the MBP-PknA (wild type) protein.

Thr-172 and Thr-174 in the Activation Loop of PknA Are the Phosphorylating Residues—Protein kinases exhibit a multitude of mechanisms for their regulation. The best understood aspect of regulation reconciled in recent years is phosphorylation on a residue(s) located in a particular segment in the center of the kinase domain, which is termed the activation segment or T-loop (32). The activation loop in several kinases has been found to be highly disordered in the crystal structure and is capable of undergoing large conformational changes when the kinase switches between active and inactive states (33). The crystal structure of PknB has highlighted the importance of the activation loop in supporting the universal activation mechanism of the kinase (18). The loop thus identified consists of two threonines actively participating in the activation of the protein (34). We therefore examined if PknA undergoes activa-

Self-association of PknA Reconstitutes Its Functionality

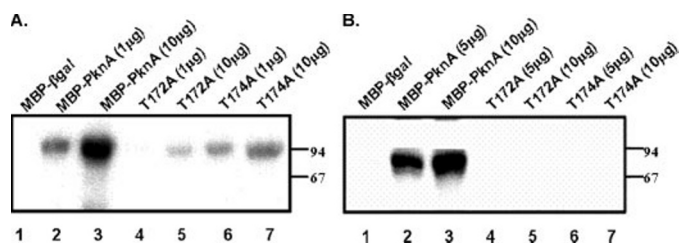


FIGURE 4. Role of threonine residues in the activation loop on autophosphorylating ability of PknA and its core. Mutants of PknA and the core (T172A, T174A) were generated. Mutant proteins were expressed and purified as outlined under "Experimental Procedures." *A*, autophosphorylating ability of the mutants of PknA was assessed using different amounts of protein in the assay. *Lane 1*, MBP- β gal control; *lane 2*, 1 μ g of MBP-PknA; *lane 3*, 10 μ g of MBP-PknA; *lane 4*, 1 μ g of MBP-T172A; *lane 5*, 10 μ g of MBP-T172A; *lane 6*, 1 μ g of MBP-T174A; *lane 7*, 10 μ g of MBP-T174A. *B*, *in vitro* kinase assay with the activation loop mutants of core. *Lane 1*, MBP- β gal control; *lane 2*, 5 μ g of MBP-Core; *lane 3*, 10 μ g of MBP-Core; *lane 4*, 5 μ g of MBP-T172A Core; *lane 5*, 10 μ g of MBP-T172A Core; *lane 6*, 5 μ g of MBP-T174A Core; *lane 7*, 10 μ g of MBP-T174A Core. Position of molecular mass markers is indicated.

tion through the same mechanism. Notably, on aligning the sequence of PknA with that of PknB, two threonines corresponding to the phosphothreonines in the activation loop of PknB were located (Fig. 1A). The modeled three-dimensional structure of PknA also showed the presence of disordered activation loop (data not shown). Interestingly, comparable threonines have also been found to exist in other mycobacterial Ser/Thr kinases, like PknD, PknE, and PknF (30).

To analyze the role of these two mapped threonines of the putative activation loop (DFGIAKAVDAAPVTQTGM-VMGTAQYIAPE) of PknA or its core (Δ 339–431) on kinase activity, they were mutated one at a time to alanine (T172A and T174A). These single mutants were purified as MBP fusion proteins, and their autophosphorylating abilities were monitored. Both the mutations affected the autophosphorylating ability of PknA (Fig. 4A). However, the effect of T172A was predominant over the T174A, as evident by the difference in signal intensity (Fig. 4A, compare *lanes 2, 4, and 6* or *3, 5, and 7*). Both the mutations, on the other hand, affected the autophosphorylating ability of the core confirming the results obtained with the full-length protein (Fig. 4B). Interestingly, the profound effect of both the mutations on the core, compared with that of the PknA, presumably point toward difference in the stability between the proteins. In PknB, replacement of both the threonines to alanine equally affected the autophosphorylating ability of the protein (33). Thus, our results establish the direct regulatory role of threonines of the activation loop in autophosphorylation of PknA and favor the universal activation mechanism of this kinase.

PknA Core Exhibits Autophosphorylation in Trans—We have reported earlier that PknA is an active eukaryotic type Ser/Thr protein kinase, and it predominantly phosphorylates at threonine residues (9). However, the biochemical mechanism underlying phosphorylation is poorly understood. Available literature indicates that autophosphorylation of protein kinases occur either through an intramolecular (*cis*) or intermolecular (*trans*) association (35). To resolve the underlying mechanism of autophosphorylation of PknA, we tested the ability of the protein to phosphorylate its inactive version. For this purpose, full-length protein (MBP-PknA) was mixed with increasing

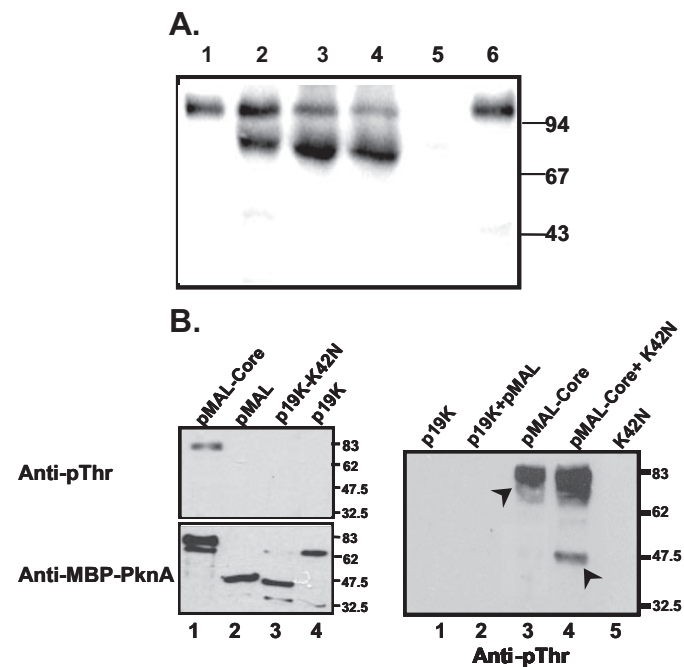


FIGURE 5. Trans-autophosphorylation of PknA. *A*, 2 μ g of MBP-PknA was incubated with 0 (*lane 1*), 4 (*lane 2*), 8 (*lane 3*), and 16 μ g (*lane 4*) of MBP-K42N Core and 16 μ g (*lane 6*) of MBP- β gal. *Lane 5* indicated 16 μ g of MBP-K42N Core. *B*, *in vivo* trans-autophosphorylation of core. *E. coli* cells transformed with different constructs were subjected to Western blotting as detailed under "Experimental Procedures." *Left panel*, *E. coli* cells transformed with single plasmids pMAL-Core (*lane 1*), pMAL (*lane 2*), p19K-K42N (*lane 3*), and vector p19Kpro (*lane 4*) were immunoblotted with anti phosphothreonine (*anti-pThr*, upper panel) and anti-MBP-PknA antisera (*lower panel*). *Right panel*, cells co-transformed with p19Kpro and pMAL vectors (*lane 2*), pMAL-Core and p19Kpro-K42N (*lane 4*), cells transformed with p19Kpro (*lane 1*), pMAL-Core (*lane 3*), and p19Kpro-K42N (*lane 5*) were immunoblotted with anti-phosphothreonine antibody (*anti-pThr*). Position of molecular mass markers is indicated. Expressed proteins (Core and K42N) are denoted with arrowheads.

concentrations (2–8-fold excess) of a kinase-inactive version of PknA core carrying altered Mg^{2+} -ATP orienting lysine to asparagine (MBP-Core-K42N), and the samples were subjected to kinase assay. As shown in Fig. 5A, the K42N mutant, which is unable to autophosphorylate itself (*lane 5*), undergoes phosphorylation on incubation with wild type protein (*lanes 2–4*). Interestingly, a decrease in the phosphate content of wild type protein on incubation with increasing concentrations of the K42N indicates that the mutant was capable of suppressing the intrinsic autophosphorylation ability of the PknA in a dose-dependent manner. However, no such compromise in the PknA phosphorylation ability could be observed when the wild type protein was incubated with an excess of the MBP- β gal (Fig. 5A, *lane 6*), which further confirmed the authenticity of this experiment.

To substantiate the intermolecular mechanism of autophosphorylation of this kinase, we carried out *in vivo* co-expression experiments in *E. coli* by transforming PknA or K42N (in p19kpro vector) along with the core (in pMAL-c2X vector). Because PknA is predominantly phosphorylated at threonine residues (9), we observed that an anti-Thr(P) antibody recognizes PknA or its core (Fig. 5B, *left upper panel*, *lane 1*) (21) but not its kinase-inactive variant K42N (Fig. 5B, *left upper panel*, *lane 3*). Loading of both the proteins was confirmed by the anti-MBP-PknA antibody in the same blot following its strip-

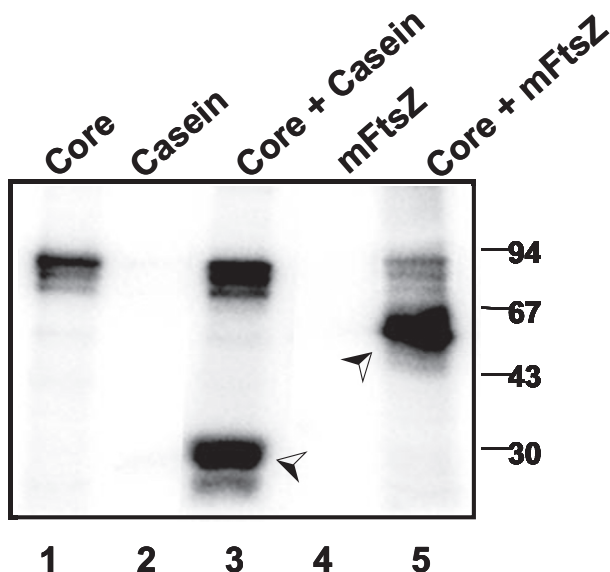


FIGURE 6. Substrate phosphorylation of PknA core. Casein or GST-mFtsZ was incubated (25 °C for 20 min) with MBP-Core in kinase buffer along with [γ - 32 P]ATP. The reaction was stopped by adding 5 \times SDS buffer, and samples were resolved in 10% SDS-PAGE and processed for autoradiography as described under "Experimental Procedures." Lane 1, MBP-Core (5 μ g); lane 2, casein (10 μ g); lane 3, casein (10 μ g) with MBP-Core; lane 4, mFtsZ (2 μ g); lane 5, mFtsZ (2 μ g) with MBP-Core. The position of molecular mass markers (in kDa) is indicated. The lane numbers are shown at the bottom. Arrowheads represent casein or mFtsZ.

ping (Fig. 5B, left lower panel, lanes 1 and 3). We found that the use of anti-Thr(P) antibody in Western blotting of cell lysates prepared from *E. coli* cells co-transformed with K42N and the PknA core recognized both the proteins (Fig. 5B, right panel, lane 4). The recognition of K42N by the antibody was specific because no phosphosignals corresponding to the mutant protein could be detected in absence of PknA core (Fig. 5B, right panel, lane 5). Thus, both the lines of evidence strongly insinuate that autophosphorylation of the PknA is a bimolecular reaction.

PknA Core Is Capable of Substrate Phosphorylation—After establishing the autophosphorylation behavior of the core region, it was tempting to envisage whether the core is able to transfer phosphate to substrates known to be phosphorylated by full-length PknA. To investigate this aspect, purified core protein was incubated with [γ - 32 P]ATP and casein. As shown in Fig. 6, in addition to an autophosphorylating band of PknA core, substrate phosphorylation was evident (lane 3). In earlier reports, we established that the cell division protein FtsZ is a natural substrate of PknA (21). To check the phosphorylation of FtsZ from *M. tuberculosis* (mFtsZ) by PknA core, kinase assay was carried out following mixing of both the proteins. As expected, in addition to PknA core a phosphorylating band corresponding to mFtsZ could be seen (Fig. 6, lane 5). These results suggest that unlike PknB and PknF (30), the juxtamembrane region encompassing residues 269–338, is indispensable not only for autophosphorylation of PknA but also for its substrate phosphorylation ability.

Interaction between Core and C-terminal Domains Is Crucial for the Functionality of PknA—Available literature indicated that in eukaryotes for functionality, different domains of Ser/

Thr protein kinases interact with each other (36). Although this aspect has not yet been elucidated in any prokaryotes, being a sensor kinase interaction between domains of PknA is expected. We therefore focused our attention to evaluate such association between the core and the C-terminal domains (transmembrane and extracellular regions) of PknA. For this purpose, although core (Δ 339–431) was tagged with MBP (MBP-Core), other domains (juxta-transmembrane, 253/363; extracellular, 363/431; and juxta-transmembrane-extracellular, Δ 1–252) were expressed as GST fusion proteins. *In vitro* interactions between them were examined in pull-down assays. The GST-tagged proteins (GST-(253/363), GST-(363/431), and GST-(Δ 1–252)) were incubated (one at a time) with MBP-Core and passed through amylose resin. As shown in Fig. 7A, Western blotting of the samples eluted from the column with anti-GST antibody highlighted GST-(253/363) as well as GST-(Δ 1–252) (upper panel) and anti-MBP antibody recognized the MBP-Core (lower panel). Surprisingly, anti-GST antibody recognized an \sim 31-kDa band in addition to GST-(Δ 1–252) (\sim 53 kDa), which seems to be a cleaved product of the fusion protein (Fig. 7A, lane 2). However, no band corresponding to the GST-(Δ 1–252) could be detected on incubating the protein with amylose resin in the absence of the MBP-Core, indicating the specificity of the interaction (Fig. 7A, upper panel, compare lanes 1 and 2). GST-(363/431), on the other hand, showed negligible interaction with the MBP-Core protein (Fig. 7A, upper panel, lane 3). The results of the *in vitro* interaction studies were further confirmed in solid phase binding assays (see "Experimental Procedures"). As shown in Fig. 7B, following affinity purification, binding of biotinylated MBP-Core and GST-(253/363) or GST-(Δ 1–252) exhibited a saturation kinetics (half-maximal binding = \sim 4 ng/ml; dissociation constant = 0.08 ± 0.01 nM). On the other hand, GST-(363/431) exhibited hardly any binding. The binding of GST-(253/363) or GST-(Δ 1–252) could not be observed when BSA replaced the MBP-Core. Because both GST-(253/363) and GST-(Δ 1–252) indicate the interactions of PknA core with its transmembrane domain, we further monitored the ability of unlabeled GST-(Δ 1–252) to inhibit its binding of biotinylated MBP-Core (Fig. 6C). The 50% inhibition of binding was achieved at \sim 2 μ g/ml of GST-(Δ 1–252), although use of MBP- β gal (pMAL-c2 vector as negative control) had no significant effect (Fig. 7C). Although the involvement of overlapping 87 amino acids (residues 253–339 spanning the juxtamembrane region) among the constructs (core, MBP-(Δ 339–431) and GST-(253/363) or GST-(Δ 1–252)) used in this study could not be ruled out, all the lines of evidence strongly argue in favor of interaction between core and the transmembrane domain of PknA.

The role of different domains of PknA toward its functionality was further analyzed. For this purpose, a heterologous expression system was utilized. Earlier studies have already established that constitutive expression of PknA results in elongation of *E. coli* cells (9). We therefore utilized this distinguishing property of the full-length protein (p19kpro-PknA) to elucidate the interaction between different domains of PknA. Because the core emulates the catalytic activities of the wild type protein, we examined the effect of its expression on the morphology of the *E. coli* cells. Surprisingly, we found that con-

Self-association of PknA Reconstitutes Its Functionality

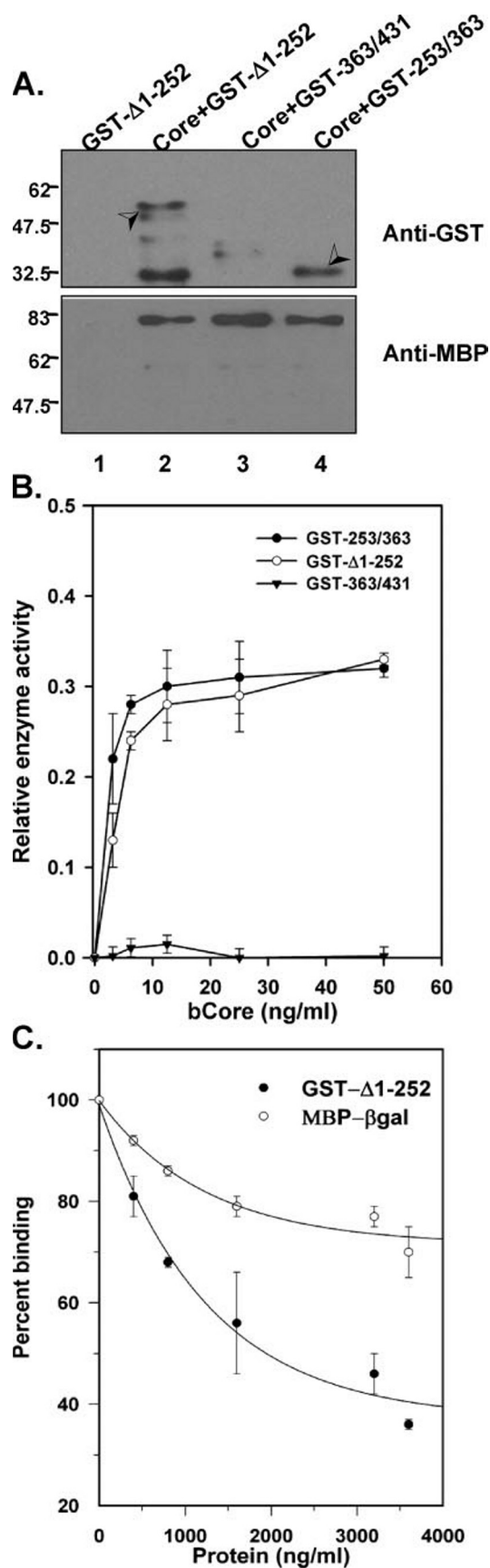


FIGURE 7. Interaction of PknA core and other domains. *A*, pull-down assay was carried out by incubating purified GST fusion proteins (GST-(253/363), GST-(363/431), and GST-(Δ1-252)) with purified MBP-Core and amylose resin

stitutive expression of p19kpro-Core did not alter the cell phenotype (Fig. 8, compare *a* and *b*). This observation together with the identification of possible *in vitro* interaction between the core and the C-terminal region, especially the transmembrane domain, led us to speculate their self-association for the functionality of the protein. Despite their *in vitro* interaction (see Fig. 7, *A* and *B*), co-transformation of the p19kpro-Core and pMAL-253/363 in *E. coli* did not restore the morphological phenotype (Fig. 8*d*). On the other hand, elongated morphology of the cells could be restored on co-expression of p19Kpro-Core and pMAL-Δ1-252 constructs (Fig. 8*f*). Furthermore, p19kpro-Core when transformed with pMAL-363/431 did not affect the cell shape (Fig. 8*e*), suggesting the importance of both transmembrane and extracellular domains in exhibiting functional reconstitution of PknA. The altered phenotype of the cells thus supported our hypothesis that the domains associate *in trans* to reconstitute a functional protein *in vivo*. However, there could still be the possibility that the genetic interaction or reconstitution was mediated by the overlapping cytoplasmic portion of the kinase, *i.e.* juxtamembrane region. To test this possibility, nonoverlapping construct pGEX-Δ1-338 (transmembrane-extracellular domains) was co-transformed with the p19Kpro-Core. Interestingly, the phenotype was restored as shown in Fig. 8*f*, *inset*. We therefore concluded that the transmembrane domain could be involved in mediating the interaction; however, signaling by complete molecule cannot take place in the absence of the sensory cues from the extracellular domain.

DISCUSSION

Protein kinases play a cardinal role in phosphorylation of proteins and in the process regulate a variety of crucial activities in prokaryotes as well as in eukaryotes. In recent years, genes for eukaryotic type phospho-signaling system were identified in bacteria, and several studies are now focused on unraveling their physiological roles (37). In this scenario, we concentrated on PknA, one of the 11 such Ser/Thr protein kinases present in the genome of the dreadful pathogen *M. tuberculosis*. PknA has been implicated in playing a role in regulating morphological changes associated with cell division (9, 21). Like any other bacterial eukaryotic type Ser/Thr protein kinases, although the

in binding buffer with 10 mM glutathione. The proteins were extracted from the beads using sample buffer as described under "Experimental Procedures" and analyzed by immunoblotting with anti-glutathione *S*-transferase (*anti-GST*; upper panel) and anti-MBP (*lower panel*) antibodies. Lane 1, GST-(Δ1-252) incubated with amylose resin in the absence of MBP-Core; lane 2, GST-(253/363) with MBP-Core; lane 3, GST-(363/431) with MBP-Core; lane 4, GST-(Δ1-252) with MBP-Core. *B*, binding of GST fused domains with MBP-Core. Different deletion constructs of PknA (GST-(253/363), GST-(363/431), GST-(Δ1-252); 1 μg/well) were coated on microtiter plates, washed, and incubated in the presence of the indicated concentrations of biotinylated MBP-Core (*bCore*) as described under "Experimental Procedures." Following addition of streptavidin-HRP, enzyme activity of each well was monitored to quantitate binding. The relative enzyme activity was calculated after subtracting the blank (well coated with 1 μg of BSA) and expressed as mean ± S.D. from three independent experiments. *C*, competition of MBP-Core binding. The binding of biotinylated core (25 ng/well) with immobilized GST-(Δ1-252) was determined. The HRP activity in the absence of any competitor was taken as 100%, and the results (mean ± S.D., *n* = 3) are expressed as percentage of biotinylated core bound to GST-(Δ1-252). Arrowheads represent GST-(Δ1-252) or GST-(253/363).

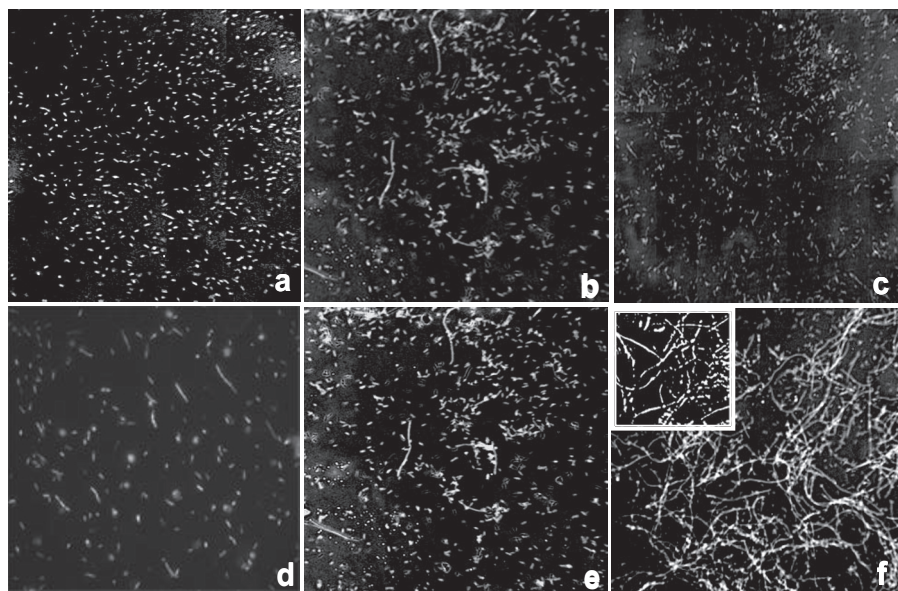


FIGURE 8. Reconstitution of functionality of PknA by co-expression of different domains. *E. coli* (DH5 α) cells were co-transformed with different plasmid constructs as mentioned under "Experimental Procedures." Morphology of cells was determined by phase contrast microscopy after staining with methylene blue. Cells co-transformed with p19Kpro and pMAL vectors (a), p19Kpro-Core (b), pMAL- Δ 1-252 (c), p19Kpro-Core and pMAL-253/363 (d), p19Kpro-Core and pGEX-363/431 (e), p19Kpro-Core and pMAL-(Δ 1-252) (f). *Inset*, cells co-transformed with p19Kpro-Core and pGEX- Δ 1-338.

presence of catalytic, juxtamembrane, transmembrane, and extracellular domains has been revealed in PknA through bioinformatic analysis, how the domains collaborate with each other toward its functionality is not yet known. We therefore concentrated on the structure-function analysis of this kinase, especially concentrating on the identification of region responsible for the catalytic activity, its mechanism of activation, and finally to evaluate interaction between different domains for the functionality of PknA.

Sequence alignment, as well as the modeled three-dimensional structure of PknA, has indicated its high order of homology with the catalytic domains of PknB (Figs. 1A and 2). However, in the juxtamembrane regions of the two kinases, the similarity is considerably less (Fig. 1A). Full-length PknA (431 amino acid residues) has been shown to exhibit autophosphorylation as well as substrate phosphorylation abilities (4). The truncation of the protein to cytosolic region harboring catalytic and juxtamembrane domains did not hamper such activities and behaved similarly in respect to the effect of divalent cations (Fig. 3B) or inhibitors (Figs. 1C, 3, and 6). However, unlike PknB and PknF (30), further trimming the protein to the catalytic domain alone completely abolished the enzymatic activity of PknA (Figs. 1C and 2B). Strikingly, the homology shared by the juxtamembrane region rich in alanine and proline with that of the Ala/Ser/Thr/Pro/Gly region of Pkn2, the Ser/Thr protein kinase from *Myxococcus xanthus* (38), and its requirement for the catalytic activity, corroborate well with our phylogenetic prediction earlier (9). Thus, from this study it is apparent that the catalytic domain along with the juxtamembrane region are the minimum spans required for autophosphorylation as well as substrate phosphorylation abilities of PknA and together constitute the "catalytic core." Although such an indispensability of the juxtamembrane region so far has not been reported for

any mycobacterial Ser/Thr kinase, its involvement in activation of several eukaryotic kinases is well known. For instance, in receptor tyrosine kinases and transforming growth factor- β receptor Ser/Thr kinase, the juxtamembrane region serves as a key auto-inhibitory element regulating kinase activity (39). In human epidermal growth factor receptor, the juxtamembrane region has been shown to be indispensable for allosteric kinase activation and productive monomer interactions within a dimer (40). In this scenario, our observation may point toward a dimerization interface in the juxtamembrane region of PknA, distinct from that already predicted in its catalytic domain (15), imparting the kinase activity. Furthermore, it can also be hypothesized that the juxtamembrane region constituting part of the core could be involved in providing

structural integrity or stability to the kinase. Nonetheless, the indispensability of the juxtamembrane region seems to be a distinctive feature of PknA, which led us to elucidate the regulation of catalytic activity as well as its functionality.

It is well known that most of the kinases control phosphorylation status through the activation loop. Sequence comparison has identified certain structural determinants explaining the reason behind their activation through phosphorylation. It has been suggested that kinases containing a catalytic aspartate preceded by an arginine residue, termed as RD kinases, are known to be activated by phosphorylation in the activation segment (33). Analysis of the PknA sequence revealed the presence of RD motif, suggesting the existence of a parallel mechanism of activation as has been observed with PknB (20). Interestingly, we also identified the activation segment carrying the two predicted phosphorylating threonines on the basis of sequence alignment with PknB (Fig. 1A). We therefore mutated these two threonines and as expected could identify Thr-172 and Thr-174 as the phosphorylating residues (Fig. 4). Thus, it could be predicted that activation of PknA occurs by a universal activation mechanism like other eukaryotic kinases (32).

Autophosphorylation of Ser/Thr kinases in eukaryotes is known to occur either by the *cis* or *trans* mechanism (41, 42). In fact, very little information is available regarding the mechanism of autophosphorylation of bacterial Ser/Thr kinases. To have an insight on this aspect, *in vitro* phosphorylation assays were performed utilizing the kinase-active and -inactive versions of full-length and PknA core, respectively. It is apparent from the experiment depicted in Fig. 5 that the autophosphorylation occurs *in trans*. Furthermore, *in vivo* phosphorylation of the full-length kinase-inactive mutant (p19Kpro-K42N) by the co-expressed kinase-active core (pMAL-Core) emphasized the prevalence of intermolecular autophosphorylation of PknA

Self-association of PknA Reconstitutes Its Functionality

(Fig. 5B). Thus, our results ostensibly established that the PknA exhibits bimolecular autophosphorylation like the majority of histidine kinases in bacteria and most of the eukaryotic receptor kinases (43–45).

Previously we have reported that PknA, when expressed in *E. coli* under a constitutive promoter, resulted in cell elongation (9). Surprisingly, the core, which is enzymatically active, upon transformation in *E. coli* was unable to bring about phenotypic changes (Fig. 8b) as has been observed with the full-length protein. It was therefore hypothesized that there could be a prevalence of interaction/association between different domains of PknA, which may lead to phenotypic changes. To test this possibility, the core was co-transformed with either transmembrane or extracellular domain. Both the core and transmembrane domains were found to interact *in vitro* (Fig. 7); however, co-transformation of the two did not restore the phenotype, indicating the insufficiency of the transmembrane domain alone in reconstitution of the functionality of PknA (Fig. 8d). On the other hand, co-transformation of the extracellular domain along with core neither showed any interaction (Fig. 7) nor any phenotypic change (Fig. 8e). Interestingly, co-expression of core with the transmembrane and regulatory regions exhibited interaction (Fig. 7) as well as restored the elongation phenotype (Fig. 8f, inset), suggesting association of these domains in *trans* and reconstitution of a fully active protein in this heterologous setting. All these observations therefore indicated the indispensability of the domains for reconstitution of the functionality of PknA and therefore the prevalence of a distinct mechanism for this kinase. Such self-association and functional reconstitution have also been reported for a Ser/Thr protein kinase fused (Fu), a component of Hedgehog signaling complex in *Drosophila* (36). Alternatively, the interdomain interaction/association might have restored the ability of PknA to recognize regulatory cues that lead to its transformation from inactive to active state through conformational changes as has been reported for transforming growth factor- β receptor Ser/Thr kinase (39).

Finally, our results for the first time signify the importance of each domain of a bacterial eukaryotic type Ser/Thr kinase toward reconstitution of its functionality. All these lines of evidence underscore the molecular mechanism of regulation of PknA and hence may provide an insight into the mechanism of signal transduction in mycobacteria.

Acknowledgments—We gratefully acknowledge the kind gift of expression vector p19Kpro from Drs. D. B. Young and M. Blokpoel, Imperial College School of Medicine at St. Mary's London, UK. We thank Dr. S. Karthikeyan for help in structure superimposition. We are thankful to J. Prasad for providing us with excellent technical assistance.

REFERENCES

- Hunter, T. (2000) *Cell* **100**, 113–127
- West, A. H., and Stock, A. M. (2001) *Trends Biochem. Sci.* **26**, 369–376
- Ginsberg, A. M., and Spigelman, M. (2007) *Nat. Med.* **13**, 290–294
- Cole, S. T., Brosch, R., Parkhill, J., Garnier, T., Churcher, C., Harris, D., Gordon, S. V., Eglmeier, K., Gas, S., Barry, C. E., III, Tekaia, F., Badcock, K., Basham, D., Brown, D., Chillingworth, T., Connor, R., Davies, R., Devlin, K., Feltwell, T., Gentles, S., Hamlin, N., Holroyd, S., Hornsby, T., Jagels, K., Krogh, A., McLean, J., Moule, S., Murphy, L., Oliver, K., Osborne, J., Quail, M. A., Rajandream, M. A., Rogers, J., Rutter, S., Seeger, K., Skelton, J., Squares, R., Squares, S., Sulston, J. E., Taylor, K., Whitehead, S., and Barrell, B. G. (1998) *Nature* **393**, 537–544
- Av-Gay, Y., and Everett, M. (2000) *Trends Microbiol.* **8**, 238–244
- Greenstein, A. E., Grundner, C., Echols, N., Gay, L. M., Lombana, T. N., Miecskowski, C. A., Pullen, K. E., Sung, P., and Alber, T. (2005) *J. Mol. Microbiol. Biotechnol.* **9**, 167–181
- McCarty, D. R., and Chory, J. (2000) *Cell* **103**, 201–209
- Koul, A., Choidas, A. K., Tyagi, A. K., Drlica, K., Singh, Y., and Ulrich, A. (2001) *Microbiology* **147**, 2307–2314
- Chaba, R., Raje, M., and Chakraborti, P. K. (2002) *Eur. J. Biochem.* **269**, 1078–1085
- Molle, V., Girard-Blanc, C., Kremer, L., Doublet, P., Cozzzone, A. J., and Prost, J. (2003) *Biochem. Biophys. Res. Commun.* **308**, 820–825
- Molle, V., Kremer, L., Girard-Blanc, C., Besra, G. S., Cozzzone, A. J., and Prost, J. F. (2003) *Biochemistry* **42**, 15300–15309
- Gopalaswamy, R., Narayanan, P. R., and Narayanan, S. (2004) *Protein Expression Purif.* **36**, 82–89
- Sharma, K., Chandra, H., Gupta, P. K., Pathak, M., Narayan, A., Meena, L. S., D'Souza, R. C., Chopra, P., Ramachandran, S., and Singh, Y. (2004) *FEMS Microbiol. Lett.* **233**, 107–113
- Walburger, A., Koul, A., Ferrari, G., Nguyen, L., Prescianotto-Baschong, C., Huygen, K., Klebl, B., Thompson, C., Bacher, G., and Pieters, J. (2004) *Science* **304**, 1800–1804
- Greenstein, A., Echols, E. N., Lombana, T. N., King, D. S., and Alber, T. (2007) *J. Biol. Chem.* **282**, 11427–11435
- Canova, M. J., Veyron-Churlet, R., Zanella-Cleon, I., Cohen-Gonsaud, M., Cozzzone, A. J., Becchi, M., Kremer, L., and Molle, V. (2008) *Proteomics* **8**, 521–533
- Kang, C. M., Abbott, D. W., Park, S. T., Dascher, C. C., and Cantley, L. C. (2005) *Genes Dev.* **19**, 1692–1704
- Villarino, A., Duran, R., Wehenkel, A., Fernandez, P., England, P., Brodin, P., Cole, S. T., Zimny-Arndt, U., Jungblut, P. R., Cervenansky, C., and Alzari, P. M. (2005) *J. Mol. Biol.* **350**, 953–963
- Ortiz-Lombardia, M., Pompeo, F., Boitel, B., and Alzari, P. M. (2003) *J. Biol. Chem.* **278**, 13094–13100
- Young, T. A., Delagoutte, B., Endrizzi, J. A., Falick, A. M., and Alber, T. (2003) *Nat. Struct. Biol.* **10**, 168–174
- Thakur, M., and Chakraborti, P. K. (2006) *J. Biol. Chem.* **281**, 40107–40113
- Ho, S. N., Hunt, H. D., Horton, R. M., Pullen, J. K., and Pease, L. R. (1989) *Gene (Amst.)* **77**, 51–59
- Yang, W., Zhang, L., Lu, Z., Tao, W., and Zhai, Z. (2001) *Protein Expression Purif.* **22**, 472–478
- Sambrook, J., Fritsch, E. F., and Maniatis, T. (1989) *Molecular Cloning: A Laboratory Manual*, 2nd Ed., pp. 1.82–1.84, Cold Spring Harbor Laboratory Press, Cold Spring Harbor, NY
- Bradford, M. M. (1976) *Anal. Biochem.* **72**, 248–254
- Thompson, J. D., Gibson, T. J., Plewniak, F., Jeanmougin, F., and Higgins, D. G. (1997) *Nucleic Acids Res.* **25**, 4876–4882
- McGuffin, L. J., Bryson, K., and Jones, D. T. (2000) *Bioinformatics (Oxf)* **16**, 404–405
- Schwede, T., Koppl, J., Guex, N., and Peitsch, M. C. (2003) *Nucleic Acids Res.* **31**, 3381–3385
- Sierk, M. L., and Kleywegt, G. J. (2004) *Structure (Lond.)* **12**, 2103–2111
- DeLano, W. L. (1998) *The PyMOL Molecular Graphics System*, DeLano Scientific LLC, San Carlos, CA
- Duran, R., Villarino, A., Bellinzoni, M., Wehenkel, A., Fernandez, P., Boitel, B., Cole, S. T., Alzari, P. M., and Cervenansky, C. (2005) *Biochem. Biophys. Res. Commun.* **333**, 858–867
- Nolen, B., Tylor, S., and Ghosh, G. (2004) *Mol. Cell* **15**, 661–675
- Johnson, L. N., Noble, M. E. M., and Owen, D. J. (1996) *Cell* **85**, 149–158
- Boitel, B., Ortiz-Lombardia, M., Duran, R., Pompeo, F., Cole, S. T., Cervenansky, C., and Alzari, P. M. (2003) *Mol. Microbiol.* **49**, 1493–1508
- Oliver, A. W., Knapp, S., and Pearl, L. H. (2007) *Trends Biochem. Sci.* **32**, 351–356
- Ascano, M., and Robbins, D. J. (2004) *Mol. Cell Biol.* **24**, 10397–10405

Self-association of PknA Reconstitutes Its Functionality

37. Deutscher, J., and Saier, M. H. (2005) *J. Mol. Microbiol. Biotechnol.* **9**, 125–131
38. Udo, H., Munoz-Dorado, J., Inouye, M., and Inouye, S. (1995) *Genes Dev.* **9**, 972–983
39. Huse, M., Chen, Y. G., Massague, J., and Kuriyan, J. (1999) *Cell* **96**, 425–436
40. Thiel, K. W., and Carpenter, G. (2007) *Proc. Natl. Acad. Sci. U. S. A.* **104**, 19238–19243
41. Park, S. Y., Avraham, H. K., and Avraham, S. (2004) *J. Biol. Chem.* **279**, 33315–33322
42. Rogers, J. A., Read, R. D., Li, J., Peters, K. L., and Smithgall, T. E. (1996) *J. Biol. Chem.* **271**, 17519–17525
43. Lammers, R., Obberghena, E. V., Ballotti, R., Schlessinger, J., and Ullrich, A. (1990) *J. Biol. Chem.* **265**, 16886–16890
44. Cai, S. J., and Inouye, M. (2003) *J. Mol. Biol.* **329**, 495–503
45. Iuchi, S. (1993) *J. Biol. Chem.* **268**, 23972–23980